

# Frequency-dependent hydrodynamic inductance and the determination of the thermal and quantum noise of a superfluid gyroscope

Talso Chui and Konstantin Penanen

*Jet Propulsion Laboratory, California Institute of Technology, Pasadena, California 91109, USA*

(Received 13 January 2005; published 25 April 2005)

We reexamine mass flow in a superfluid gyroscope containing a superfluid Josephson weak link. We introduce a frequency-dependent hydrodynamic inductance to account for an oscillatory flow of the normal fluid component in the sensing loop. With this hydrodynamic inductance, we derive the thermal phase noise, and hence the thermal rotational noise of the gyroscope. We examine the thermodynamic stability of the system based on an analysis of the free energy. We derive a quantum phase noise, which is analogous to the zero-point motion of a simple harmonic oscillator. The configuration of the studied gyroscope is analogous to a conventional superconducting RF SQUID. We show that the gyroscope has very low intrinsic noise ( $1.9 \times 10^{-13} \text{ rad s}^{-1}/\sqrt{\text{Hz}}$ ), and it can potentially be applied to study general relativity, Earth science, and to improve global positioning systems (GPS).

DOI: 10.1103/PhysRevB.71.132509

PACS number(s): 67.40.-w, 05.70.Ln, 67.57.Bc, 74.50.+r

The practical use of quantum interference has become widespread with the development of the superconducting interference device (SQUID). The recent discovery of the Josephson effect in superfluids<sup>1-3</sup> makes a very sensitive superfluid gyroscope a possibility. Already, Simmonds *et al.*<sup>4</sup> and Mukharsky *et al.*<sup>5</sup> have demonstrated gyroscopes based on this effect. With sufficient resolution, a potential geodesy application of this device is for real-time precise measurement of the Earth's rotation speed. Jitter in Earth's rotation is a source of uncertainty in real-time GPS. From the very long baseline interferometry measurements of Hide and Dickey,<sup>6</sup> the Earth's rotation jitter causes an equivalent position jitter of  $\sim 10$  cm at the equator in a day. Precise measurement of the jitter in real time will allow this error to be removed. Another potential application is in tests of general relativity by precise measurement of the geodetic and the frame dragging precession. Understanding the fundamental limits of these gyroscopes is therefore of both scientific and practical interest. In the following, we extend an earlier concept of the fluctuations of the quantum phase<sup>7</sup> to treat the superfluid gyroscope. We consider a readout scheme in which the rotation rate is inferred from the measurement of the resonant frequency of small-amplitude oscillations in a resonator (inset of Fig. 1) formed by a flexible diaphragm, a Josephson weak link, and a sensing loop of  $N_L$  turns. We find that in a typical geometry, the normal component undergoes oscillatory motion and is not viscously clamped to the walls of the gyroscope's sensing loop. We treat the normal fluid flow by introducing a frequency-dependent hydrodynamic inductance. We then explore how it affects the noise and stability of the gyroscope.

The flow of the normal component is coupled to the oscillatory superfluid flow through mass conservation. The current driven by the diaphragm of area  $A$  is  $\rho A \dot{x}$ , where  $\rho$  is the fluid density and  $x$  is the displacement of the diaphragm from equilibrium, positive if displaced upward in Fig. 1. Both the normal fluid velocity  $u_n$  and  $x$  are oscillatory, while the superfluid velocity  $u_s$ , the phase difference  $\phi$  across the Josephson junction, and the phase difference  $\phi_L$  across the

sensing loop have both a dc component, denoted by a subscript “o,” and an oscillatory component, denoted by a tilde over the variable. Thus  $\phi = \phi_o + \tilde{\phi}$ , where  $\phi_o$  is a dc phase bias due to a steady rotational rate  $\Omega$ , and  $\tilde{\phi}$  denotes an oscillatory component due to diaphragm oscillations. The Josephson-Anderson equation relates  $x$  to  $\tilde{\phi}$  by  $(\hbar/m)\dot{\tilde{\phi}} = -\Delta\mu = -\Delta P/\rho = -\kappa x/(\rho A)$ , where  $\Delta P$  is the pressure difference across the junction, and the contribution of temperature difference to  $\Delta\mu$  is neglected. The mass current driven by the diaphragm is therefore  $-\rho^2 A^2 \kappa_o \dot{\tilde{\phi}}/(2\pi\kappa)$ . Assuming an ideal Josephson current-phase relation, the current through the junction with a critical current  $I_c$  is  $I_c \sin \phi$ , where  $\phi$  for clockwise flow is positive. The superfluid and normal fluid current in the sense loop are  $\rho_s u_s a$  and  $\rho_n u_n a$ , where  $a$  is the cross-sectional area, and  $\rho_s, \rho_n$  are the superfluid and normal fluid densities. Since the normal fluid velocity is not uniform over the cross-sectional area,  $u_n$  is understood to be an averaged value. Mass conservation requires that

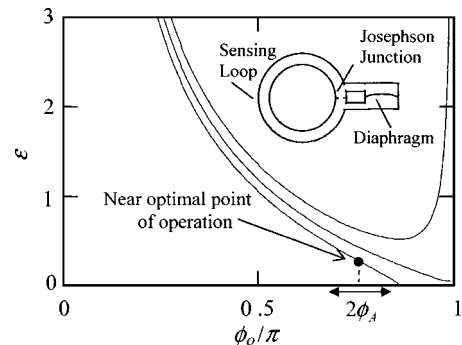


FIG. 1. The  $\varepsilon(\phi_o)$  function contains the  $\phi_o$  dependent of  $\Delta\Omega$  in Eq. (11). The top, middle, and bottom lines are for  $\beta_o = 0.9, 0.999$ , and  $1.1$ , respectively. The inset shows the three components of a superfluid gyroscope. The sensing loop has  $N_L$  turns, but only one turn is shown.

$$-\rho^2 A^2 \kappa_o \ddot{\phi} / (2\pi\kappa) = I_c \sin \phi + \rho_s u_s a + \rho_n u_n a + \gamma' \dot{\phi}\text{-drive}, \quad (1)$$

where the term  $\gamma' \dot{\phi}$  is due to all dissipative processes other than that due to normal fluid flow. The dissipative current due to normal fluid flow is already included as  $i\rho_n \text{Im}(u_n)a$ . A sinusoidal current drive term is also added to keep the oscillator's steady-state amplitude constant; at resonance the drive term is imaginary. For oscillatory flow at frequency  $f$ , the extent of normal fluid flow in a tube of diameter  $d$  depends on the viscous penetration depth  $\lambda = \sqrt{\eta/(\pi\rho_n f)}$ , where  $\eta$  is the viscosity of the normal fluid. For superfluid  $^4\text{He}$  (Ref. 8) near the lambda transition,  $\lambda = 74 \mu\text{m}/\sqrt{f}$ . For superfluid  $^3\text{He}$  (Ref. 9) at  $\sim 0.5$  mK,  $\lambda \approx 1 \text{ cm}/\sqrt{f}$ . At high frequencies, where  $\lambda \ll d$ , the fluid undergoes solid body motion, where  $u_n = \tilde{u}_s$ . At low frequencies where  $\lambda \gg d$ , the normal fluid is clamped to the walls, and  $u_n = 0$ . Since  $u_n$  is oscillatory, one can write  $u_n = \alpha \tilde{u}_s$ , where  $\alpha$  is a proportionality constant. Thus  $\alpha \rightarrow 0$  for low frequencies, and  $\alpha \rightarrow 1$  for high frequencies; in both limits the flow is dissipationless. At intermediate frequencies,  $\alpha$  is complex;  $\text{Im}(\alpha)$  accounts for the dissipation. We write  $\rho_s u_s a + \rho_n u_n a = \rho_s u_{s0} a + \rho_L \tilde{u}_s a + i\rho_n \tilde{u}_s a \text{Im}(\alpha)$ , where  $u_{s0}$  is the dc component of  $u_s$ , and  $\rho_L = \rho_s + \text{Re}(\alpha)\rho_n$  is an effective density of fluid participating in nondissipative motion. We also define a total dissipation parameter  $\gamma$  that includes dissipation due to normal fluid flow, so that  $\gamma\dot{\phi} = \gamma' \dot{\phi} + i\rho_n \tilde{u}_s a \text{Im}(\alpha)$ . Equation (1) becomes

$$-\rho^2 A^2 \kappa_o \ddot{\phi} / (2\pi\kappa) = I_c \sin \phi + \rho_s u_{s0} a + \rho_L \tilde{u}_s a + \gamma\dot{\phi}\text{-drive}. \quad (2)$$

It is possible to express  $u_s$  in terms of  $\phi_L$ , using the relation  $u_s = \kappa_o \nabla \Phi / (2\pi)$ , and identifying  $\nabla \Phi = \phi_L / \ell$ , where  $\Phi$  is the quantum phase of the superfluid wave function,<sup>7</sup>  $\ell$  is the length of the sensing loop, and  $\kappa_o = h/m$  is a quantum of circulation,  $h$  is Planck's constant, and  $m$  is the mass of a  $^4\text{He}$  atom or the mass of a Cooper pair in  $^3\text{He}$ . For sensing loops of  $N_L$  turns with radius  $R$ ,  $\ell = 2\pi N_L R$ . Thus  $\rho_s u_{s0} a = -I_c \phi_{L0} / \beta_o$ , where  $\beta_o = 2\pi L_o I_c / \kappa_o$  is the hysteresis parameter<sup>10,11</sup> as in RF SQUID, and  $L_o = \ell / (a\rho_s)$  is the ordinary superfluid hydrodynamic inductance. The term  $\rho_L \tilde{u}_s a$  can be written as  $-I_c \tilde{\phi}_L / \beta_L$ , where  $\beta_L = 2\pi L_L I_c / \kappa_o$ , and  $L_L = \ell / (a\rho_L)$  is the frequency-dependent hydrodynamic inductance. At low frequencies  $L_L \rightarrow L_o$ . At high frequencies  $L_L \rightarrow L_\infty$ , where  $L_\infty = \ell / (a\rho)$ , and  $\beta_L \rightarrow \beta_\infty$ , where  $\beta_\infty = 2\pi L_\infty I_c / \kappa_o$ . We obtain

$$-\rho^2 A^2 \kappa_o \ddot{\phi} / (2\pi\kappa) = I_c \sin \phi - I_c \phi_{L0} / \beta_o - I_c \tilde{\phi}_L / \beta_L + \gamma\dot{\phi}\text{-drive}. \quad (3)$$

The sum of  $\phi$  and  $\phi_L$  is related to  $\Omega$ . To obtain this relation, we note that in a superfluid, while the relation  $u_s = (\kappa_o / 2\pi) \nabla \Phi$  is applicable in a rotating laboratory frame, the quantization condition  $(2\pi / \kappa_o) \oint u_s d\ell = 2\pi M$ , where  $M$  is an integer or zero, must be applied in an inertial frame (a reference frame that is not rotating). The velocity  $u'_s$  in an inertial frame is related to the velocity  $u_s$  in the laboratory frame by  $u'_s = u_s - \Omega R$ . Performing the integral around

a closed loop, in the zeroth quantum state ( $M=0$ ) we obtain  $(2\pi / \kappa_o) \oint (u_s - \Omega R) d\ell = \phi_L - \phi_x + \phi = 0$ , where  $\phi_L = (2\pi / \kappa_o) \oint u_s d\ell$ , the integral across the Josephson junction gives  $\phi$ , while  $\phi_x = (2\pi / \kappa_o) \oint (\Omega R) d\ell = 2\pi N_L \Gamma / \kappa_o$ , where  $\Gamma = 2\Omega \pi R^2$  is the circulation. Using  $\phi_L = \phi_x - \phi$ , and making the expansion  $\phi = \phi_o + \tilde{\phi}$ , Eq. (3) becomes

$$-\rho^2 A^2 \kappa_o \ddot{\tilde{\phi}} / (2\pi\kappa) = I_c \sin(\phi_o + \tilde{\phi}) + I_c(\phi_o - \phi_x) / \beta_o + I_c \tilde{\phi} / \beta_L + \gamma \dot{\tilde{\phi}}\text{-drive}. \quad (4)$$

The dc phase  $\phi_o$  can be found by setting drive,  $\dot{\tilde{\phi}}$ ,  $\ddot{\tilde{\phi}}$ , and  $\tilde{\phi}$  to zero. We then expand around  $\phi_o$  to obtain the equation of motion and the resonant frequency. The results are

$$\sin \phi_o + (\phi_o - \phi_x) / \beta_o = 0, \quad (5)$$

$$[\rho^2 A^2 \kappa_o / (2\pi\kappa)] \ddot{\tilde{\phi}} + I_c [\cos \phi_o + 1 / \beta_L] \tilde{\phi} + \gamma \dot{\tilde{\phi}} = \text{drive}, \quad (6)$$

$$f_o^2 = f_{oo}^2 (\cos \phi_o + 1 / \beta_L), \quad (7)$$

where  $f_{oo}^2 = \kappa I_c / (2\pi\kappa_o \rho^2 A^2)$  is the resonance frequency if the sensing loop is blocked. Notice that the crossover frequencies for  $\lambda \approx d$  in a tube of 1 cm diameter are  $\sim 55 \mu\text{Hz}$  and  $\sim 1 \text{ Hz}$  for  $^4\text{He}$  and  $^3\text{He}$ , respectively, while experimental  $f_o$  is 10–100 Hz. One should use  $\beta_\infty$  for evaluating  $f_o$ . Prior to this work, normal fluid flow was ignored<sup>12</sup> and  $\beta_o$  was used in Eq. (7), which predicts a much lower  $f_o$  near the phase transition.

Next, we derive the noise of the gyroscope by a procedure similar to that for the displacement noise in a spring-mass oscillator.<sup>13</sup> The Langevin equation in  $\tilde{\phi}$  can be obtained by replacing the drive in Eq. (6) with a Langevin equivalent noise source  $I_\delta$ ,

$$[\rho^2 A^2 \kappa_o / (2\pi\kappa)] \ddot{\tilde{\phi}} + I_c [\cos \phi_o + 1 / \beta_L] \tilde{\phi} + \gamma \dot{\tilde{\phi}} = I_\delta. \quad (8)$$

Since the thermodynamic conjugate<sup>7</sup> of  $\phi$  is  $\hbar i_s$ , where  $i_s = I_s / m$  is the superfluid particle number current,  $\hbar i_s$  is the conjugate force to the generalized displacement  $\phi$ . We multiply Eq. 8 by  $\hbar / m$  to transform it into a balance of the generalized force. Comparing this to the spring-mass system,<sup>13</sup> the power spectral density of the Langevin force maps into  $\hbar^2 i_{\delta\omega} i_{\delta\omega}^* = 4k_B T (\gamma \hbar / m)$ , and thus  $I_{\delta\omega} I_{\delta\omega}^* = 4k_B T (\gamma m / \hbar)$ , where a subscript “ $\omega$ ” on a variable denotes its Fourier transform. Following the spring-mass oscillator case,<sup>13</sup> the power spectral density of  $\phi$  and the variance of  $\phi$  are

$$\phi_\omega \phi_\omega^* = \frac{2k_B T [\pi f_o Q \hbar i_c (\cos \phi_o + 1 / \beta_L)]}{[1 - (f/f_o)^2]^2 + [f/(f_o Q)]^2}, \quad (9)$$

$$(\Delta \phi_{rms})^2 = \int_0^\infty \phi_\omega \phi_\omega^* df = k_B T / [\hbar i_c (\cos \phi_o + 1 / \beta_L)], \quad (10)$$

where  $Q = \rho^2 A^2 \kappa_o \omega_o / (2\pi\gamma\kappa)$  and assuming  $\beta_L = \beta_\infty$ . To derive an expression relating  $\Delta \phi_{rms}$  to the noise in the measurement of  $f_o$ , we assume that the oscillator is driven at fre-

quency  $f_o$ , so that at steady state,  $\tilde{\phi} = \phi_A \cos(\omega_o t + \theta)$ , where  $\phi_A$  is an amplitude and  $\theta$  is a phase lag. Thermal noise of  $\phi$  can be decomposed into an amplitude noise in  $\phi_A$  and a phase noise in  $\theta$ . Only the phase noise contributes to the error in frequency determination. The noise energy is divided equally between the amplitude and the phase fluctuations. The single side-band phase noise is  $\mathcal{L}(f_m) = (1/2)\phi_\omega(f_o + f_m)\phi_\omega^*(f_o + f_m)/(\phi_A/\sqrt{2})^2$ . For  $Q \gg 1$ ,  $\mathcal{L}(f_m) \approx 2\tau_o(\Delta\phi_{rms}/\phi_A)^2/(1+4\pi^2\tau_o^2f_m^2)$ , a Lorentzian noise spectrum, where  $\tau_o = 2Q/\omega_o$  is the oscillator's ring-down time. By integrating  $\theta_\omega(f_m)\theta_\omega^*(f_m) = 2\mathcal{L}(f_m)$ , we obtain  $(\Delta\theta_{rms})^2 = (\Delta\phi_{rms}/\phi_A)^2$ . Alternatively, one can represent the oscillator's motion without noise by a unit vector rotating with an angle of  $\omega_o t$  on a graph where the  $x$  axis is  $\phi/\phi_A$  and the  $y$  axis is  $\dot{\phi}/(\omega_o\phi_A)$ . The result  $(\Delta\theta_{rms})^2 = (\Delta\phi_{rms}/\phi_A)^2$  is due to  $\Delta\theta = \Delta\dot{\phi} \cos(\omega_o t + \theta)/(\omega_o\phi_A) - (\Delta\phi/\phi_A)\sin(\omega_o t + \theta)$ . Since two measurements of  $\theta$  separated by a time interval  $t$  much shorter than  $\tau_o$  are correlated, their difference  $\Delta\theta(t)$  should tend to zero as  $t \rightarrow 0$ . We have shown by numerical simulation that for Lorentzian noise,  $\Delta\theta(t) = \Delta\theta_{rms}\sqrt{2t/\tau_o}$  as  $t \rightarrow 0$ . Now let the drive be turned off at time  $t=0$ , and a measurement begin where the time of zero crossing is measured to determine the period. After a time  $t \ll \tau_o$ , the accumulated error in the time of zero crossing is  $\Delta t = \Delta\theta(t)/\omega_o = (\Delta\theta_{rms}/\omega_o)\sqrt{2t/\tau_o}$ . The uncertainty in  $f_o$  for one such measurement is  $\Delta f_1 = f_o \Delta t/t = \Delta\phi_{rms}\sqrt{2}/(\tau_o t)/(2\pi\phi_A)$ . After time  $t$ , the oscillator is re-excited and the measurement is repeated for  $N$  times for a total measurement time of  $\tau = Nt$ . The error in the frequency is reduced to  $\Delta f = \Delta f_1/\sqrt{N} = \Delta\phi_{rms}\sqrt{2}/(\tau_o\tau)/(2\pi\phi_A)$ . It is possible to make a free running oscillator using feedback. A feedback scheme, which introduces an energy pulse at the zero crossings, will not affect the phase evolution and will preserve the preceding expression for  $\Delta f$ . Using Eqs. (5), (7), and (10), and the relations  $\phi_x = (2\pi)^2 N_L \Omega R^2 / \kappa_o$  and  $\Delta\Omega = (d\Omega/d\phi_x)(d\phi_x/d\phi_o)(d\phi_o/df_o)\Delta f$ , we obtain

$$\Delta\Omega = \frac{\kappa_o}{4N_L R^2} \sqrt{\frac{2k_B T}{\pi^5 f_{oo} Q \hbar i_c \tau}} \frac{\varepsilon(\phi_o, \beta_o)}{\phi_A}, \quad (11)$$

$$\varepsilon(\phi_o, \beta_o) = \beta_o [\cos \phi_o + 1/\beta_L]^{1/4} (\cos \phi_o + 1/\beta_o) / \sin \phi_o, \quad (12)$$

where  $1/\beta_L \approx 1/\beta_\infty = (\rho/\rho_s)(1/\beta_o)$ . Since  $\rho/\rho_s > 1$ , normal fluid flow causes the noise to increase. The increase is particularly large for  $^4\text{He}$  near the lambda point. For  $u_n=0$ , a similar expression was given in Ref. 12 for a phase-sensitive detection scheme.

To explore thermodynamic stability, we write the free energy as<sup>7,14,15</sup>  $dF = \hbar i_c \sin \phi d\phi + a\ell\rho_s u_s du_s + a\ell u_n d(\rho_n u_n) + A\ell_1 \dot{x} d(\rho \dot{x}) + \kappa x dx$ , where  $\ell_1$  is an effective length of the drive chamber. Writing  $u_s$  in terms of  $\phi$ , we obtain

$$dF = \hbar i_c [\sin \phi + (\phi - \phi_x)/\beta_o] d\phi + \ell u_n dI_n + \ell_1 \dot{x} dI_x + \kappa x dx, \quad (13)$$

where  $I_n = \rho_n u_n a$  and  $I_x = \rho \dot{x} A$ . We notice that during the oscillation, thermodynamic equilibrium is maintained, because

$f_o$  is much lower than  $1/\tau_{LK}$ , where  $\tau_{LK}$  (the Landau-Khalatnikov time) is the time scale for equilibration. Both  $I_n$  and  $I_x$  can be considered as constant at any instant. This implies that the total superfluid current  $I_{s,total} = mi_c [\sin \phi + (\phi - \phi_x)/\beta_o]$  must also be constant. Therefore, the stability condition<sup>7,14</sup> is  $(\partial I_{s,total}/\partial \phi) = (\partial^2 F/\partial \phi^2)_{I_n, I_x} > 0$ , leading to  $\cos \phi > -1/\beta_o$ . When  $\beta_o < 1$ , this condition is satisfied for all possible values of  $\phi$ , and the system is stable. However, when  $\beta_o > 1$ , there are regions of  $\phi$  where this condition is violated. When this happens, the system can jump spontaneously to another stable quantum state. For  $\beta_o > 1$ , it is possible to have small-amplitude oscillations, but as the amplitude increases, at some point  $\phi$  enters the unstable region and a jump will occur. Therefore, the amplitude of the oscillations is limited. At the instability point,  $I_{s,total}(\phi)$  has a maximum. Notice that the stability condition is unchanged by the normal component flow. However, contrary to prior work,  $f_o$  does not tend to zero at the instability point [Eq. (7)]. Instead, it tends to  $f_{oo}(\rho_n/\rho_s)(1/\beta_o)$ .

At small amplitudes, the equation of motion of  $\tilde{\phi}$  is similar to that of a simple harmonic oscillator. There should be a quantum noise in  $\tilde{\phi}$  which is analogous to the zero point motion of the displacement  $z$  given by  $\langle z^2 \rangle = \hbar/(m_z \omega_o)$ , where  $m_z$  is the mass. By analogy,  $\langle \phi^2 \rangle = \hbar/(m_\phi \omega_o)$ , where  $m_\phi$  is a generalized mass. To find  $m_\phi$ , we multiply Eq. (8) by  $\hbar/m$  to transform it into a balance of the generalized force. By analogy, the coefficient of the  $\ddot{\phi}$  term is  $m_\phi = \kappa_o^2 \rho^2 A^2 / (4\pi^2 \kappa)$ . We obtain  $\langle \phi^2 \rangle = 2\pi f_{oo} / (i_c \sqrt{\cos \phi_o + 1/\beta_L})$ . The rotational quantum noise can be obtained by replacing the thermal noise  $\Delta\phi_{rms}$  in Eq. (11) by the quantum noise.

We have expressed all quantities in terms of an effective nondissipative fluid density  $\rho_L = \rho_s + \rho_n \text{Re}(\alpha)$ , where  $\alpha = u_n/\tilde{u}_s$ . For intermediate frequencies,  $\alpha$  can be determined as follows: Since  $\tilde{u}_s = (\hbar/m)(\tilde{\phi}_L/\ell)$  and  $\Delta P = -(\hbar\rho/m)\tilde{\phi}_L$ , one can write  $\Delta P = -i\omega\rho\ell\tilde{u}_s$ . The normal fluid experiences a partial pressure of  $(\rho_n/\rho)\Delta P$ . With this, one can solve the Navier-Stokes equation numerically to determine the normal fluid velocity profile as a function of  $\tilde{u}_s$ , and hence determine  $\alpha$ .

To optimize the gyroscope, we plot  $\varepsilon(\phi_o, \beta_o)$  of Eq. (12) in Fig. 1, where  $\phi_o$  can be set by tilting the axis of the gyroscope relative to the axis of rotation. It diverges at  $\phi_o = 0$  and  $\pi$ , where  $df_o/d\phi_o = 0$  according to Eq. (7). One should avoid operating near these points. The top, middle, and bottom lines are for  $\beta_o = 0.9, 0.999$ , and  $1.1$ , respectively, for  $\rho/\rho_s = 2$ . For  $\beta_o > 1$  (bottom line), it appears that  $\varepsilon \rightarrow 0$  at the instability point where  $(\cos \phi_o + 1/\beta_o) \rightarrow 0$ . As one approaches this point,  $\phi_A$  must also be reduced to avoid jumps. Thus, the relevant figure of merit,  $\varepsilon/\phi_A$ , approaches a constant. For example, setting  $\phi_o = 0.75\pi$  and  $\phi_A = 0.08\pi$  as shown by the thick dot, we obtain  $\varepsilon/\phi_A \approx 1$ . For  $\beta_o < 1$  (top line),  $\varepsilon(\phi_o)$  has a minimum within the range of  $0$  to  $\pi$ . As  $\beta_o \rightarrow 1$ , the minimum is lower and it occurs closer to  $\pi$ . If one operates near the minimum, the available range for linear oscillation is also reduced. Again,  $\varepsilon/\phi_A$  or  $\Delta\Omega$  approaches a constant. For  $\phi_o = 0.9\pi$  and  $\phi_A = 0.07\pi$ , one obtains  $\varepsilon/\phi_A \approx 0.8$ .

We estimate the noise of a superfluid  $^3\text{He}$  gyroscope by

assuming that  $\varepsilon/\phi_A \approx 1$  and  $\beta_o=1$ . At  $T/T_c=0.5$ , where  $T_c=0.929$  mK, Backhaus *et al.*<sup>16</sup> reported that the critical current is  $I_c=0.093$   $\mu\text{gm/s}$  or  $i_c=9.3 \times 10^{15}/\text{s}$ . This  $I_c$  and  $T$  implies that the following design would give  $\beta_o=1$ :  $N_L=1$ ,  $R=7.5$  cm, and  $a=1$  cm<sup>2</sup>. We further assume that  $\kappa$  is set to give  $f_{oo}=100$  Hz, and that  $Q=100$ . From Eq. (11), we obtain a rotational rate noise density of  $\sqrt{\Omega_\omega \Omega_\omega^*}=2.6 \times 10^{-9} \Omega_E/\sqrt{\text{Hz}}$ , where  $\Omega_E$  is the Earth's rotation rate. It should be noted that the diaphragm displacement noise is  $x_\omega x_\omega^*=(f\kappa_o \rho A/\kappa)^2 \phi_\omega \phi_\omega^*=10^{-30}$  m<sup>2</sup>/Hz at  $f_o$ . This value is achievable with SQUID electronics. For comparison, the quantum noise in  $\Omega$  is  $6.3 \times 10^{-13} \Omega_E$ , the geodetic and frame-dragging precessions are  $\sim 6.6 \times 10^{-9} \Omega_E$  and  $\sim 6.6 \times 10^{-11} \Omega_E$ , respectively, and the Earth's rotational jitter is  $\sim 2.5 \times 10^{-9} \Omega_E$ . In conclusion, we have shown that at its fundamental limit, the gyroscope can potentially be applied to study general relativity, Earth science, and to improve GPS.

As a side note, the frequency-dependent hydrodynamic

inductance may have other important implications. For example, Davis and Packard<sup>17</sup> suggested that the ratio of hydrodynamic inductances of the weak link to that of the sensing loop, also known as the  $R$  ratio, should exhibit a strong increase as one approaches the superfluid transition due to suppression of the superfluid density by the finite-size effect in the weak link. It was not understood why the data of Sukhatme *et al.*<sup>3</sup> did not show such an increase. We notice that the  $R$  ratio is the same as  $1/\beta_L$ , and should therefore also be a frequency-dependent quantity. The decrease in  $\rho_L$  at reduced frequency may partially cancel the depression by the finite-size effect in the weak link, providing a plausible explanation

We thank Professor Goodstein for helpful comments on thermodynamic stability. This work was carried out at the Jet Propulsion Laboratory, California Institute of Technology, under a contract with NASA.

<sup>1</sup>O. Avenel and E. Varoquaux, Phys. Rev. Lett. **60**, 416 (1988).

<sup>2</sup>S. Backhaus, S. V. Pereverzev, A. Loshak, J. C. Davis, and R. E. Packard, Science **278**, 1435 (1997).

<sup>3</sup>K. Sukhatme, Y. Mukharsky, T. Chui, and D. Pearson, Nature (London) **411**, 280 (2001).

<sup>4</sup>R. W. Simmonds, A. Marchenkov, E. Hoskinson, J. C. Davis, and R. E. Packard, Nature (London) **412**, 55 (2001).

<sup>5</sup>Y. Mukharsky, O. Avenel, and E. Varoquaux, Physica B **280**, 287 (2000).

<sup>6</sup>R. Hide and J. O. Dickey, Science **253**, 629 (1991).

<sup>7</sup>T. Chui, W. Holmes, and K. Penanen, Phys. Rev. Lett. **90**, 085301 (2003).

<sup>8</sup>G. Ahlers, in *The Physics of Liquid and Solid Helium, Part I*, edited by K. H. Bennemann and J. B. Ketterson (Wiley, New York, 1976), p. 176.

<sup>9</sup>M. Nakagawa, A. Matsubara, O. Ishikawa, T. Hata, and T. Kodama, Phys. Rev. B **54**, R6849 (1996).

<sup>10</sup>A. H. Silver and J. E. Zimmerman, Phys. Rev. **157**, 317 (1967).

<sup>11</sup>B. Chesca, J. Low Temp. Phys. **110**, 963 (1998).

<sup>12</sup>O. Avenel, Yu. Mukharsky, and E. Varoquaux, J. Low Temp. Phys. **135**, 745 (2004).

<sup>13</sup>P. R. Saulson, Phys. Rev. D **42**, 2437 (1990).

<sup>14</sup>T. C. P. Chui, D. L. Goodstein, A. W. Harter, and R. Mukhopadhyay, Phys. Rev. Lett. **77**, 1793 (1996).

<sup>15</sup>D. L. Goodstein, *States of Matter* (Dover, New York, 1985), p. 336.

<sup>16</sup>S. Backhaus, S. V. Pereverzev, A. Loshak, J. C. Davis, and R. E. Packard, Science **278**, 1435 (1997).

<sup>17</sup>J. C. Davis and R. E. Packard, Rev. Mod. Phys. **74**, 741 (2002).